

Supporting information

Enhanced adsorption of cage-shaped proteins on carbon surface by CNT binding peptide aptamer

Narangerel Ganbaatar^{1*}, Ting-Chieh Chu¹, Naofumi Okamoto², Kenji Iwahori¹, Masakazu Nakamura², and Ichiro Yamashita^{1*}

¹*Graduate School of Engineering, Osaka University, 2-8 Yamadaoka, Suita, Osaka 565-0871, Japan*

²*Division of Materials Science, Nara Institute of Science and Technology, Ikoma, Nara 630-0192, Japan*

E-mail: yamashita@jrl.eng.osaka-u.ac.jp, narangerel@jrl.eng.osaka-u.ac.jp

1. QCM electrode preparation
2. Carbon Surface characterization
3. Protein preparation
4. QCM batch-mode experiments
5. Dissociation constant calculation

1. QCM electrode preparation

First, commercially available gold-electrode QCM sensors (QA-A9M-AU(M)(SEP), Seiko EG&G) were cleaned by rinsing with milli-Q water and ethanol at least 3 times, followed by drying with dry nitrogen gas. After cleaning, carbon deposition was carried out on the cleaned sensors using a vacuum deposition machine (CADE-E).

A carbon fiber mesh sheet was used as the carbon source which was able to make a uniform carbon thin film by vapor deposition. First, the carbon fiber mesh was set between the electrodes in the vacuum chamber, then, the QCM sensors were set against it, and a shutter was inserted between them. In this configuration, a 10-second preheating process was performed to remove

surface impurities. Next, the shutter was opened and an electric current was applied to the carbon fiber mesh for Joule heating. The current value was set to ~35A. By this heating, a carbon thin film was deposited on the QCM sensors in a short time (1.7 seconds). After deposition, the QCM sensors were rinsed with the milli-Q water which remove the unnecessary deposited carbon film.

2. Carbon Surface characterization

Ultra-High Resolution Field Emission Scanning Electron Microscope (UHR FE-SEM, Hitachi SU9000) was used to observe the surface of the carbon-coated QCM sensor. Figure S1 shows the surface of the QCM sensor before and after the carbon deposition. The surface of the QCM gold electrode showed slight grain irregularities. After carbon deposition, the morphology of the underlying gold electrode was slightly observed in the SEM photograph. No large bump formations or grains were observed.

Figure. S1.

Raman (Laser Raman Spectrophotometer, NRS-4100-30) measurements were performed with an excitation light of 532 nm and a beam diameter was 1 μm . Measurements were taken at several locations, and the obtained spectra were almost identical. A typical result is shown in Fig. S2. The result was a broad peak (in red line). The G and D band peaks, which are characteristic of carbon materials, were not separated. Since the broadening of the peaks was induced by the low crystallinity of the carbon material in the layer, the crystal structures of the deposited carbon layer were distorted and considered to have many defects. Peak separation of the broad peak was performed, and G and D bands were extracted, respectively (in blue lines). The G band peak was around 1524 cm^{-1} , and the D band was around 1362 cm^{-1} . The G band was slightly larger than the D band, suggesting that the carbon structure with sp^2 bonds was marginally more than sp^3 at the top surface of the carbon film.

Figure. S2.

3. Protein preparation

Six kinds of cage-shaped proteins were used: 4 types of mutant cage-shaped proteins with CNT binding peptide aptamers on the outer surface, a protein with nano-horn binding peptides (CNHB-Dps), and wild protein (w-Dps).

The *E. coli* was transformed by the plasmid, which coded the Dps subunit for the experiments. After cultivation, we harvested *E. coli* pellets and suspended them with Tris-HCl. All proteins were extracted by ultrasonic homogenization. The total protein solution was heat treated and centrifuged to remove the low heat tolerance proteins as a pellet. Proteins in the supernatant were further purified by an ion exchange column (HiTrap™ Q HP 5 ml) with an ion gradient from 0 to 0.5 M NaCl. The purity of the obtained protein was confirmed by SDS polyacrylamide gel electrophoresis (SDS-PAGE). Purified protein was further purified by gel filtration, confirmed to be of a single size, sterilized by filtering, and stored at 4°C until use. For the QCM measurements, the protein solutions were carefully prepared using milli-Q water as the solvent.

Figure S1 summarizes the characteristics of Y1 and Y2. These peptide aptamers were obtained by phage display method, targeting Meijo-D-CNT (Meijo Nano Carbon Co. Ltd., Japan). The top row shows the amino acid sequence, and the second row is a ribbon model of the 3D structure predicted by computer calculation using the PEP-FOLD3 program (University of Paris, France) with hydrophobicity shown in red. The third row shows the surface model with positive charges in blue and negative charges in red, the fourth row shows the surface model by hydrophobicity, and the bottom row shows the hydrophobicity scoring.

Peptide adsorption measurements on carbon electrodes (Screen printed electrode) were performed by EIS measurements using a PBS solution with 1 mM $[\text{Fe}(\text{CN})_6]^{3-/4-}$ mediator. To this solution, the Y1, Y2, and also the N- and C-terminal 12 amino acid sequences of Dps (DpsN, DpsC), were added sequentially at 1, 3, 10, 30, and 10 $\mu\text{g/mL}$. By fitting the obtained EIS spectra to a Randall circuit, the charge transfer resistance (R_{ct}) which was in proportional to the peptide adsorption was extracted. Figure S3 shows the results. The vertical axis is normalized using the initial R_{ct0} . Y1 had the highest adsorption ability, followed by Y2. DpsN, and DpsC had the lowest adsorption capacity.

Figure. S3.

Figure. S4

4. QCM batch-mode experiments

The profiles of frequency changes in the QCM batch-mode shown in Figure 5 were described in details here. In the first step, the chamber is filled with milli-Q water to stabilize the system. The stabilized frequency is defined as the protein-free baseline. After stabilization, milli Q water was replaced by the protein solution (0.1 mg/ml), and the protein was adsorbed onto the carbon surface. As a result, the frequency decreased from its initial baseline. After the frequency stabilized, the measurement was suspended, the protein solution was removed. Then milli-Q water was injected to wash away excess adsorbed proteins on the sensor. The increase in frequency observed in this step is due to the removal of weakly binding proteins to the surface. This protein addition and washing with milli-Q water was repeated three times. Each time, resonance frequency change (ΔF), from the stabilized initial frequency to the frequency after washing, was measured, and three ΔF values were averaged.

Quantitative differences can be seen between the adsorption of proteins with selected aptamers (Y1Ct, Y1Nt, and Y2Ct) and the others, Dps with carbon nano-horn binding aptamers (CNHB-Dps) and Dps without aptamers (w-Dps). For aptamer-modified proteins, Y1Ct, Y1Nt and Y2Ct, the frequency change was found to be 110.95 Hz, 127.9 Hz and 97.5 Hz, respectively, while for w-Dps and CNHB-Dps, the frequency change was 24.17 Hz and 58.07 Hz, respectively. The ΔF was converted to the Δm using the Sauerbrey equation (1). Δm was 39 ng/cm² (0.039 μ g/cm²) for Y1Ct, 46 ng/cm² (0.046 μ g/cm²) for Y1Nt, 35 ng/cm² (0.035 μ g/cm²) for Y2Ct, 21 ng/cm² (0.021 μ g/cm²) for CNHB-Dps and 8 ng/cm² (0.008 μ g/cm²) for w-Dps. The results showed that Y1Nt had the highest adsorption, followed by the Y1Ct and Y2Ct. The adsorption of CNHB-Dps was, and much smaller for w-Dps.

Although the above measurements clearly show differences, to minimize the effects of variation and enable more accurate quantitative discussions, the batch mode experiment was repeated 10 times and the average of 30 ΔF values was used to calculate the amount of adsorption for each protein. All ΔF and Δm data for each protein are shown in Table S1.

Table S1.

5. Dissociation constant calculation

To quantitatively evaluate the adsorption of mutant Dps on carbon substrates, the dissociation constant (K_d) was calculated.

The K_d is defined as follows using the concentration of unreacted A, B and complex AB.

$$K_d = \frac{[A][B]}{[AB]} \quad (1)$$

In the case of Dps adsorption, A is the electrode surface, B is the Dps, and AB is Dps bound on the carbon surface. K_d could be calculated by the following equations.

$$[AB] = \frac{\Delta m S}{M_w V} \quad (2)$$

$$[B] = [T] - \frac{\Delta m S}{M_w V} \quad (3)$$

$$[A] = \frac{(\Delta m_{\max} - \Delta m) S}{M_w V} \quad (4)$$

$$K_d = \frac{(\Delta m_{\max} - \Delta m) ([T] - \frac{\Delta m S}{M_w V})}{\Delta m} \quad (5)$$

where

M_w - The molecular weight of Dps,

$[T]$ - Initial concentration of Dps,

V - The volume of the reaction system,

S - The electrode area,

Δm - Amount of binding per unit area [ng/cm^2],

Δm_{\max} - Maximum binding amount (or saturated) of the electrode [ng/cm^2],

K_d - Dissociation constant [M]

In our measurements, $\frac{(\Delta m_{\max} - \Delta m) \Delta m S}{M_w V}$ is negligibly small, so the dissociation constant K_d can be expressed as follows:

$$K_d = \frac{(\Delta m_{\max} - \Delta m) [T]}{\Delta m} \quad (6)$$

Further, this relationship can be reformulated as follows.

$$\frac{[T]}{\Delta m} = \frac{[T]}{\Delta m_{\max}} + \frac{K_d}{\Delta m_{\max}} \quad (7)$$

Using equation (7) and the fitting method, we derived the K_d .

The change in the resonance frequency of the flow mode theoretically becomes the response expressed in Equation (8), where a , b , and c are constants, and t is the time.

$$\Delta f = a \cdot (1 - \exp[-t/b]) + c \quad (8)$$

The constants in equation (8) were determined by fitting the data points obtained at each protein concentration to equation (8). The saturated Δf for each protein concentration was determined. The saturated Δf can be converted to the saturated Δm using the Sauerbrey equation. After Δm values at different concentrations of Dps, $[T]$, were obtained, the data are plotted with $[T]$ on the horizontal axis and $[T]/\Delta m$ on the vertical axis to produce Figure S5. These data points must represent a linear function as seen in Equation (7). The least-squares method was used to obtain the approximate line of the linear function, and the slope and Y-intercept were obtained. Since the slope was $1/\Delta m_{\max}$, the value of Δm_{\max} could be determined. Then, the Y-intercept was $K_d/\Delta m_{\max}$ and K_d was calculated by multiplying the Y-intercept with above Δm_{\max} . Figure S5 shows the linear line obtained by the least-squares method and simultaneously the dissociation constant (K_d). K_d was found to be 1.04 μM for Y1Ct with a determination coefficient (R^2) = 0.95, 0.74 μM for Y1Nt with R^2 = 0.99, 2.18 μM for Y2Ct with R^2 = 0.98 and 3.02 μM for Y1C with R^2 = 0.94. For CNHB-Dps and w-Dps, it was difficult to calculate the K_d due to small change of resonance frequency.

Fig. S5

Figure captions

Figure. S1. The SEM images of the Au (left) and carbon-coated (right) surfaces after deposition by the vacuum deposition.

Figure. S2. Raman spectra of carbon coated QCM sensors.

Figure. S3. Predicted 3D structures of Y1 and Y2 peptide aptamers and their characteristics of hydrophobicity and charge distribution.

Figure. S4. Rct increase with peptide aptamer adsorption. Each Rct was extracted from the EIS spectrum using a Randel equivalent circuit. The obtained Rct was normalized to the initial Rct (Rct0, no peptide).

Figure. S5. Kd determination from QCM results of (a) Y1Ct, (b) Y1t, (c) Y2Ct, and (d) Y1C. Approximate straight line obtained by the least squares method from the plot of each data is displayed in circle at different concentrations.

Table S1. All ΔF and Δm obtained by the QCM batch-mode measurements.

Figures

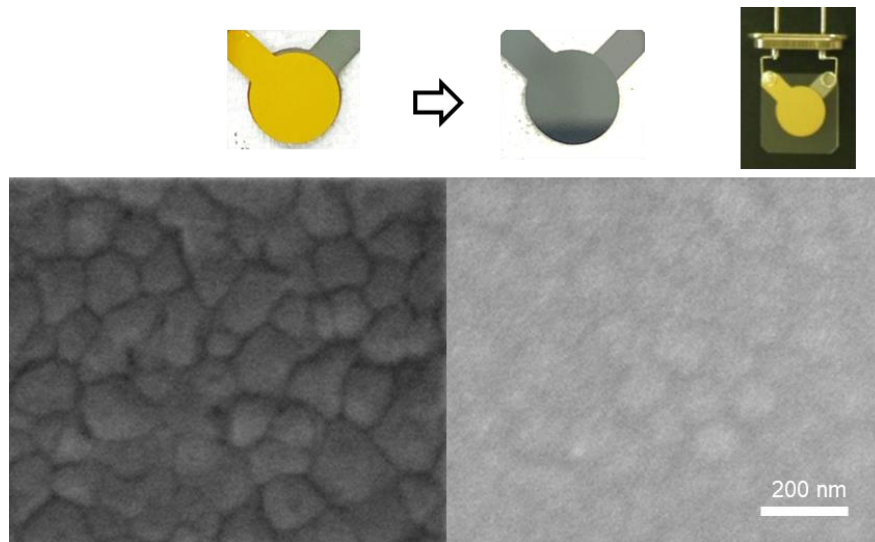


Figure S1.

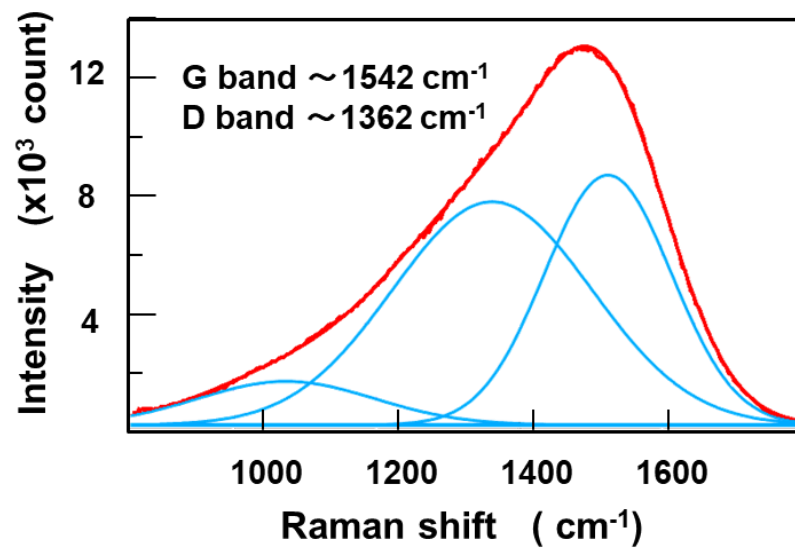


Figure S2.

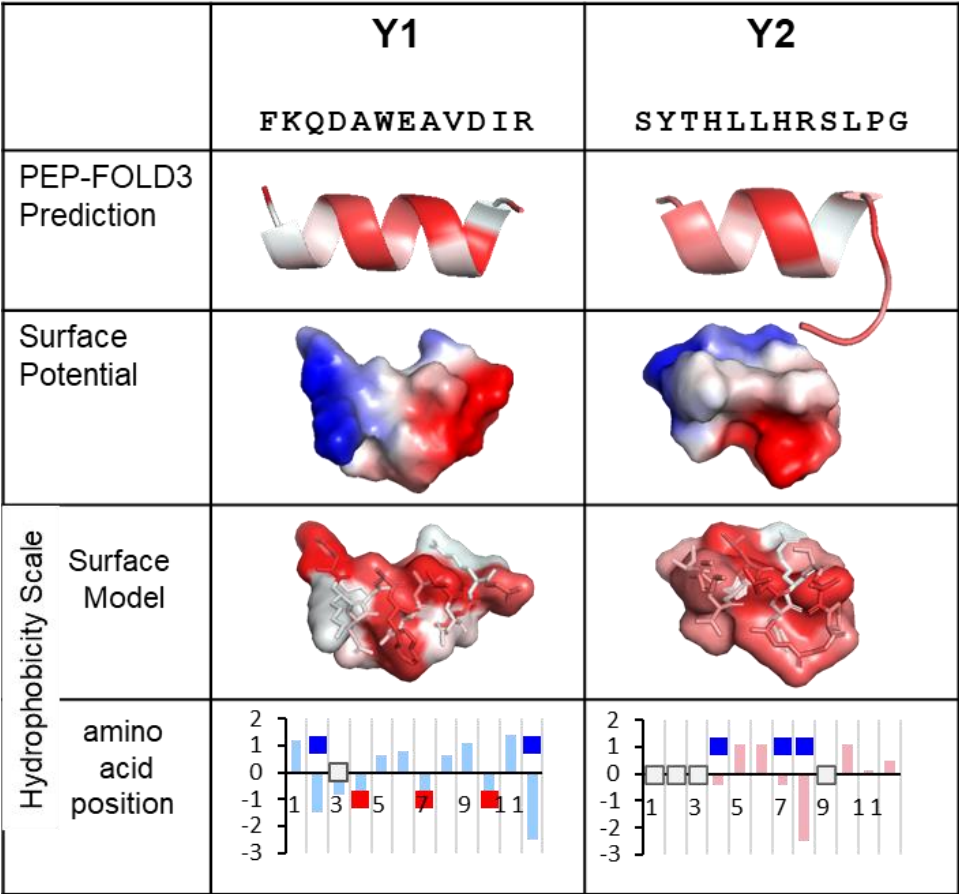


Figure S3.

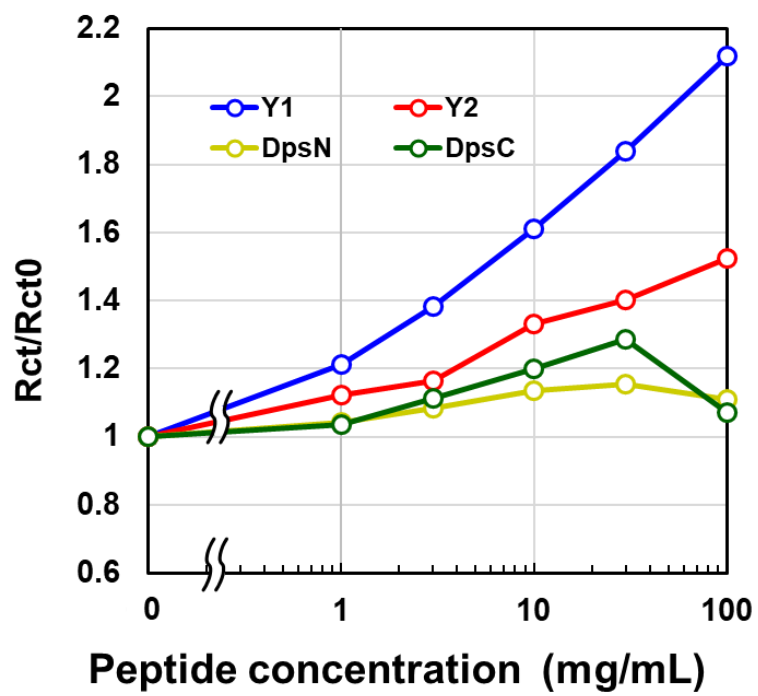


Figure S4.

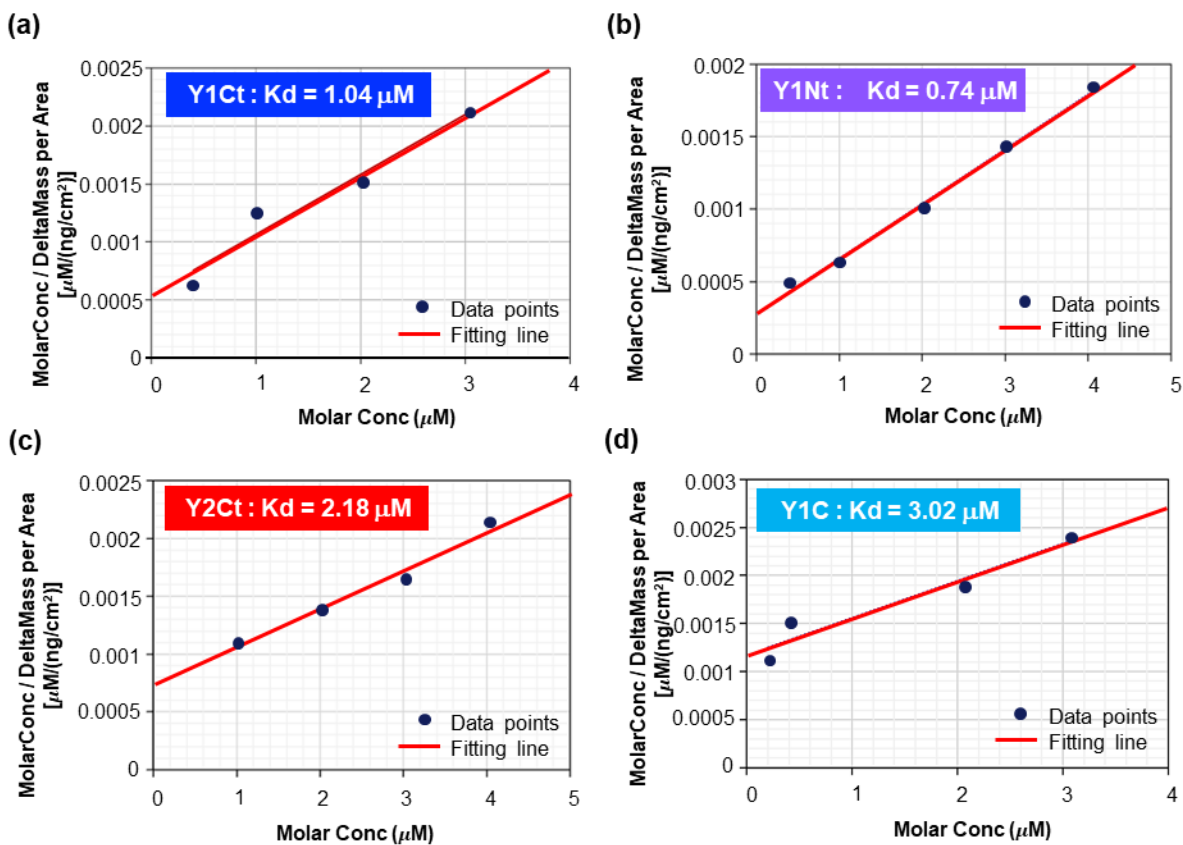


Figure S5.

Table S1.

	Y1Ct		Y1Nt		Y2Ct		CNHB-Dps		w-Dps	
	ΔF [Hz]	Δm [ng/cm ²]	ΔF [Hz]	Δm [ng/cm ²]	ΔF [Hz]	Δm [ng/cm ²]	ΔF [Hz]	Δm [ng/cm ²]	ΔF [Hz]	Δm [ng/cm ²]
1	80.84	29.10	107.69	38.77	103.64	37.31	60.20	21.67	24.08	8.67
2	122.50	44.10	177.90	64.04	130.83	47.10	61.42	22.11	7.85	2.83
3	122.33	44.04	190.02	68.41	188.90	68.00	45.71	16.45	18.02	6.49
4	77.27	27.82	95.59	34.41	91.79	33.05	51.59	18.57	32.23	11.60
5	128.37	46.21	134.76	48.51	100.84	36.30	61.78	22.24	17.61	6.34
6	178.63	64.31	145.22	52.28	91.72	33.02	60.85	21.91	34.48	12.41
7	91.71	33.01	119.58	43.05	103.66	37.32	50.31	18.11	27.34	9.84
8	97.37	35.05	117.00	42.12	127.83	46.02	70.25	25.29	23.41	8.43
9	91.80	33.05	120.13	43.25	119.56	43.04	59.30	21.35	25.09	9.03
10	87.68	31.57	147.06	52.94	93.26	33.57	68.59	24.69	29.60	10.66
11	77.94	28.06	133.79	48.16	117.00	42.12	73.26	26.37	23.09	8.31
12	99.56	35.84	145.07	52.23	82.52	29.71	77.79	28.00	27.94	10.06
13	90.06	32.42	23.53	8.47	84.41	30.39	66.74	24.03	16.75	6.03
14	120.01	43.20	89.94	32.38	93.50	33.66	66.31	23.87	35.15	12.65
15	99.26	35.73	120.86	43.51	80.82	29.10	56.13	20.21	31.46	11.32
16	95.78	34.48	120.26	43.29	97.67	35.16	71.48	25.73	14.50	5.22
17	139.15	50.09	229.03	82.45	141.96	51.10	62.56	22.52	24.19	8.71
18	125.31	45.11	108.60	39.10	102.97	37.07	57.37	20.65	25.37	9.13
19	86.20	31.03	113.93	41.01	73.12	26.32	51.88	18.68	26.54	9.55
20	94.76	34.11	112.18	40.39	87.79	31.60	42.05	15.14	22.23	8.00
21	105.59	38.01	132.41	47.67	101.71	36.61	49.75	17.91	23.49	8.46
22	108.52	39.07	120.95	43.54	69.06	24.86	76.35	27.49	22.78	8.20
23	133.73	48.14	114.51	41.22	95.54	34.39	85.83	30.90	26.43	9.52
24	99.81	35.93	165.37	59.53	85.49	30.78	49.94	17.98	19.18	6.90
25	130.67	47.04	98.27	35.38	79.17	28.50	51.05	18.38	22.53	8.11
26	130.64	47.03	127.88	46.04	79.85	28.75	56.17	20.22	39.23	14.12
27	113.89	41.00	157.57	56.73	83.42	30.03	63.12	22.72	25.59	9.21
28	108.31	38.99	186.48	67.13	82.93	29.86	50.03	18.01	29.79	10.72
29	126.78	45.64	157.51	56.71	81.20	29.23	63.74	22.95	37.19	13.39
30	114.12	41.08	140.25	50.49	82.80	29.81	42.35	15.25	28.85	10.39
Average	109.29	39.34	131.78	47.44	98.50	35.46	60.13	21.65	25.40	9.14